UCLA
UCLA Previously Published Works

Title
Self-Powered Plastron Preservation and One-Step Molding of Semiactive Superhydrophobic Surfaces

Permalink
https://escholarship.org/uc/item/5v95g2p2

Journal
Langmuir, 36(28)

ISSN
0743-7463 1520-5827

Authors
Xu, Muchen
Liu, Chunxiao Tracy
Kim, Chang-Jin

Publication Date
2020-06-26

DOI
10.1021/acs.langmuir.0c01289

Peer reviewed

eScholarship.org Powered by the California Digital Library
University of California

Accepted version for Langmuir 2020, 36, 8193−8198 https://dx.doi.org/10.1021/acs.langmuir.0c01289

Self-powered plastron preservation and one-step molding of semi-active superhydrophobic surfaces

Muchen Xu[1,*], Chunxiao "Tracy" Liu[1], and Chang-Jin "CJ" Kim[1,2,3,**]

[1]Mechanical and Aerospace Engineering Department, [2]Bioengineering Department, [3]California NanoSystems Institute (CNSI), University of California, Los Angeles (UCLA), Los Angeles, CA 90095, USA.

*Current address: 17075 Thornmint Ct, San Diego, CA 92127, USA; **Correspondence to: cjkim@ucla.edu

Abstract: Gas-trapping, mostly superhydrophobic (SHPo), surfaces are useful for underwater applications only while their plastron lasts. Because the plastron unfortunately disappears under most practical conditions, various active approaches to supply ample gas have been reported, including the semi-active SHPo surface based on self-regulated electrolysis. Here, we report two major advances: (i) self-powered plastron restoration mechanism that obviates the need for external power; (ii) one-step molding process to mass-manufacture semi-active SHPo surfaces. The advances clear major hurdles for real-world implementation.

INTRODUCTION

Trapping gas under water, textured hydrophobic surfaces, most of which being superhydrophobic (SHPo) – abbreviated to differentiate it from superhydrophilic (SHPi)[1-2] – have demonstrated great potential in many underwater applications such as drag reduction[3-5] and anti-biofouling[6]. The trapped gas, called plastron[7], may last for a long time in shallow water as found in nature[8-9] but not under typical engineering conditions due to gas diffusion[10-11], flow dynamics[12-13], and numerous environmental factors[14-17]. Since the loss of plastron would deprive SHPo surfaces of their underwater functionalities altogether, how to preserve the plastron has been the most critical issue for their underwater usage[18]. A passive approach to address the issue is to make the surface structures more robust against dewetting-to-wetting transition, such as hierarchical roughness[19-20], reentrant microstructure[21-22] and balancing pressure[23]. Textured surfaces infused with an immiscible liquid (instead of gas) would provide stability against hydrostatic pressure[24] but not against molecular diffusion (albeit slower than gas), shear drainage (more susceptible than gas)[13], etc. Although attractive because no energy is consumed, these passive approaches would have no remedy once the plastron is lost (with a rare exception[5]).

An active approach is to provide gas onto the SHPo surface and considered more practical because the plastron loss is inevitable in real-world applications[18]. The main drawbacks of the active approaches would be the energy consumption and the complexity of implementation, such as plumbing for gas distribution and wiring for electrolysis. Even though the affinity between gas bubbles and SHPo surfaces made the bubble releasing method more effective[25-26] and thermally-generated plastron worth investigating[27-29] on SHPo surfaces, their energy consumptions were still prohibitively high. Electrolysis was studied early for its relative energy efficiency[30], but it became especially attractive for SHPo surfaces when the plastron restoration was found self-regulatable[31], i.e., starting electrolysis only when and where plastron is lost and ending electrolysis as soon as plastron is restored – all automatically without any sensor or controller. This "self-regulated" or "semi-active" approach, schematically explained in Fig. 1(a), was proven with SHPo post and grating microstructures photolithographically fabricated on silicon wafer, using a DC power supply[31-32].

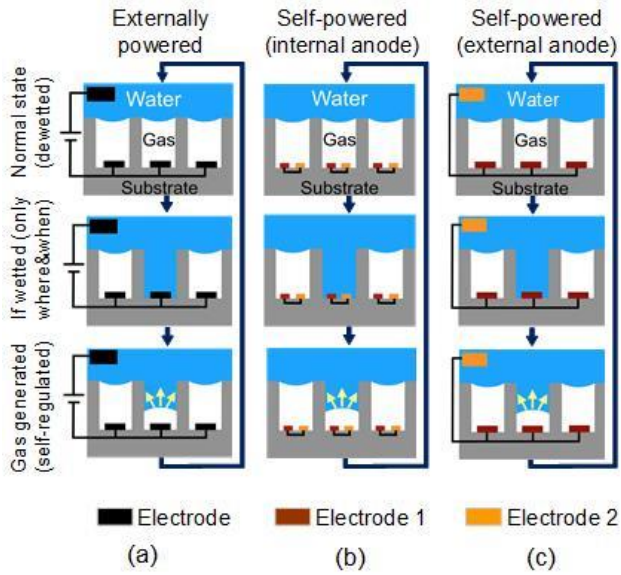

Fig. 1. Self-regulated (i.e., semi-active) plastron restoration mechanisms on a microstructured surface. (a) Using external power[31]. (b) Self-powered with both electrodes inside microstructures. (c) Self-powered with only the cathode electrode inside microstructures.

SELF-POWERED RESTORATION OF PLASTRON

The Concept. Although the self-active SHPo surface of Fig. 1(a)[31-32] is elegantly simple and the most energy efficient so far, its implementation (e.g., on boat hull) would require a power source and wiring to distribute the electricity over (often large) service areas. Aiming to make the above semi-active surface easier to implement for applications, this research paper reports two major achievements: (1) self-powering capability that would eliminate the need for and wiring to any external power source and (2) one-step hot embossing process that would fabricate the semi-active SHPo surfaces in a mass-manufacturing fashion. Figs. 1(b, c) explain the self-powered plastron restoration mechanism. Acting as two electrodes connected to each other, electrode 1 and electrode 2 are chosen from materials of two distinctively different electrode potentials. When a portion of microstructures is filled with electrolyte (e.g., seawater), which electrically connects electrode 1 and electrode 2 and shorts the circuit, a galvanic reaction ensues, and the reduction reaction on one of the two electrodes generates a gas (e.g., hydrogen) in the water. If the microstructures are designed with a proper geometry[31], the generated gas propagates laterally within the microstructures rather than forming individual bubbles that leave their surface. The criteria for lateral gas propagation inside hydrophobic microtrenches submerged in a liquid is shown below by slightly modifying and re-arranging Equation S11 of Lee and Kim[31]:

$$H / W > \frac{1+\cos\theta_{b,rec}}{2\sin\theta_{t,rec} - 2\cos\theta_{g,rec}}$$

where H is the trench depth, W is the trench width, $\theta_{b,rec}$ is the receding contact angle on the trench bottom surface, $\theta_{g,rec}$ is the receding contact angle on the trench sidewall surface and $\theta_{t,rec}$ is the receding contact angle on the trench top surface. Once the filling water is replaced with the gas, the electrochemical circuit is open and reaction stops. Unlike the semi-active mechanism of Fig. 1(a)[31], which generates the gas electrolytically, i.e., using an electrical power source as most other electrolysis approaches do, the semi-active mechanism of Figs. 1(b, c) would generate the gas spontaneously (galvanically) rather than electrolytically by an electrical power source. One may view this self-powered, self-regulated mechanism as a built-in battery consisting of an anode, a cathode, and a water electrolyte that is unused most time (while dewetted) and used occasionally (only when and where wetted).

Materials. Electrode materials selection is crucial to ensure a spontaneous gas generation when needed and no reaction otherwise. For Fig. 1(b), both cathode and anode are located inside the microstructure. In this case, firstly, the electrode potential of anode material should be smaller than that of hydrogen ion (proton) so the anode loses electrons to the hydrogen ions on cathode to generate hydrogen. Secondly, the overall cell potential, which drives the hydrogen generation on cathode, should be larger than the overpotential of hydrogen generation on cathode. However, because the anode material is consumed by the reaction but not easily replaceable inside the microstructure, we consider Fig. 1(b) as an alternative mechanism with limited utilities, such as disposable applications for short-term services. Instead, we propose Fig. 1(c) as a main mechanism, where only the cathode is located inside the microstructure to generate gas while only the anode is located outside in bulk water to provide electrons. In addition to the two requirements prescribed for Fig. 1(b) above, Fig. 1(c) requires that, thirdly, the electrode potential of cathode material should be larger than that of hydrogen ions on it so the cathode is not consumed by the reaction. Lastly, the overpotential of hydrogen generation on anode should be larger than that on cathode so hydrogen prefers to generate on cathode rather than on anode. By further restricting the materials selection to enable Fig. 1(c), note the outside anode is now easily replaceable after being consumed.

Experimental Verification. To evaluate the proposed concept of plastron preservation before embarking to develop mass-manufacturable processes, a single-trench sample was fabricated as shown in Figs. 2(a, b) by adapting the process introduced in[16, 33]. The sample was made narrow (~1 mm in width) and out of transparent Teflon FEP to allow for side-view examination of the gas restoration. Nickel and magnesium were used as cathode and anode material, respectively, in this device. The standard electrode potentials of magnesium and water are −2.37 V[34] and −0.83 V[34], respectively, while the overpotential for hydrogen evolution on nickel is ~0.2 V[35]. Since the overall cell potential of 1.54 V is higher than the overpotential for hydrogen evolution on nickel electrode (~0.2 V), spontaneous hydrogen generation is ensured. A strip of nickel foil was embedded on the bottom of the single trench and connected to a magnesium sheet placed in the surrounding water (not shown in the figure). The device was tested in seawater with the self-powered and self-regulated gas restoration process, as shown in Fig. 2(c) and Video S1. Air was trapped in the microtrench when the sample was initially submerged under seawater. When the trench was intentionally flooded using a strong jet of water (t = 0 s), the spontaneous electrochemical reaction started right away as the seawater touched the nickel electrode and closed the reaction circuit, verifying the self-initiating nature of the self-regulated plastron restoration. Similarly to what was observed by Freeman et al.[33], the generated hydrogen bubbles merged with each other to grow into larger bubbles (t = 1 s) until they reached the top edge of the trench (t = 2 s). The electrochemical reaction then stopped as the gas insulated the electrode and opened the reaction circuit, verifying the self-terminating nature of the self-regulated plastron restoration. Note the bubbles grew only laterally, never vertically off the surface, as found critical for successful self-termination[31].

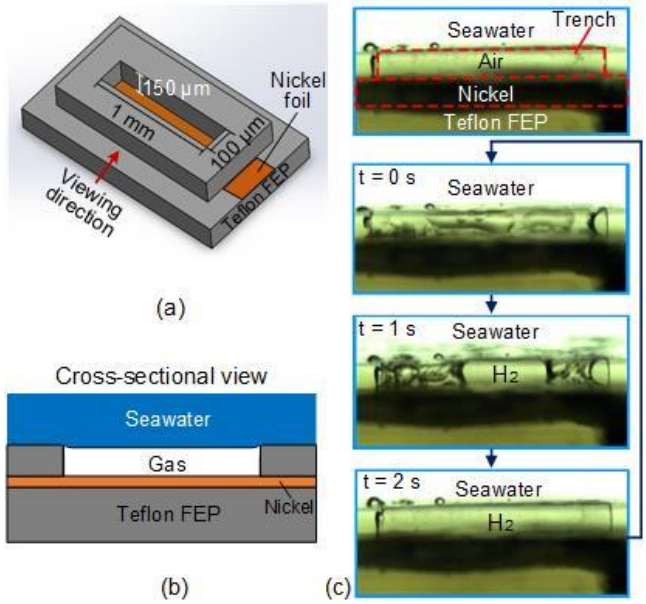

Fig. 2. Self-powered, self-regulated gas restoration process inside a single microtrench. (a) Schematic drawing of the single trench sample and dimensions. (b) Cross-sectional schematic of the sample in water. (c) Side-view snapshots of the gas restoration process. When submerged (top), air is trapped inside the trench. At t = 0 s, the air is blown out of the trench by water jet. At t = 1 s, hydrogen bubbles nucleate, merge, and propagate within the trench. At t = 2 s, plastron is restored and electrochemical reaction self-terminated.

ONE-STEP MOLDING PROCESS

As the self-powered plastron restoration mechanism confirmed above made the semi-active SHPo mechanism easier to implement, next we develop a one-step hot embossing process to fabricate the semi-active SHPo surfaces (both the existing externally powered[31-32] and the current self-powered versions) in a manner scalable for large areas and low cost. Teflon FEP was chosen as the base material due to its good thermal formability in addition to the excellent hydrophobicity and corrosion inertness expected of a PTFE material. Compared with PTFE hydrophobic coatings widely used[20, 31, 36-37], SHPo surfaces made entirely of a PTFE material would not suffer from the peeling off or deterioration of the coated thin film, making them more reliable and robust. The hot embossing process is explained in Fig. 3 and Video S2. To start, the electrodes in the form of a mesh or grating were sandwiched between a mold and a Teflon FEP film, as shown in Fig. 3(a). The reusable silicon mold was fabricated using standard semiconductor processes as detailed in Supporting Information with Fig. S1. The mold was then heated up to ~15 °C above Teflon FEP melting point (~260 °C) while pressing the Teflon FEP film against the mold at ~ 80 kPa, as shown in Fig. 3(b). A hot-embossing apparatus was custom-built as summarized in Supporting Information with Fig. S2. Note the molten Teflon FEP would flow around the electrodes and into the trenches on the mold. After the trenches were filled with the molten Teflon FEP, the hot embossing pressure was maintained while the entire hot embossing fixture (mold, Teflon FEP, and glass stock; see Fig. S3) was actively cooled down. It was found critical to keep the hot embossing pressure applied during the cooling phase to ensure the electrodes were pressed against the mold. If not, the molten Teflon FEP could seep between the electrodes and mold and cover the electrodes, interfering the electrode-water contact when the microstructure is wetted. After cooling down, the Teflon FEP film was freed from the mold, i.e., demolded, as shown in Fig. 3(c), to obtain the semi-active SHPo surface shown in Fig. 3(d), which corresponds to Figs. 1(b, c). Wire electrodes are preferred in this process so that their exposed area could be small, as shown in Fig. 3(d). Since most of metal surfaces are hydrophilic, it is desired to minimize the electrode exposure, whose hydrophilic property would hinder the desired gas propagation inside the hydrophobic trench[31]. In addition, an ample space is desired between electrodes so that the molten polymer flows around the electrodes easily to fill the trenches on the mold as shown in Fig. 3(b) and Video S2.

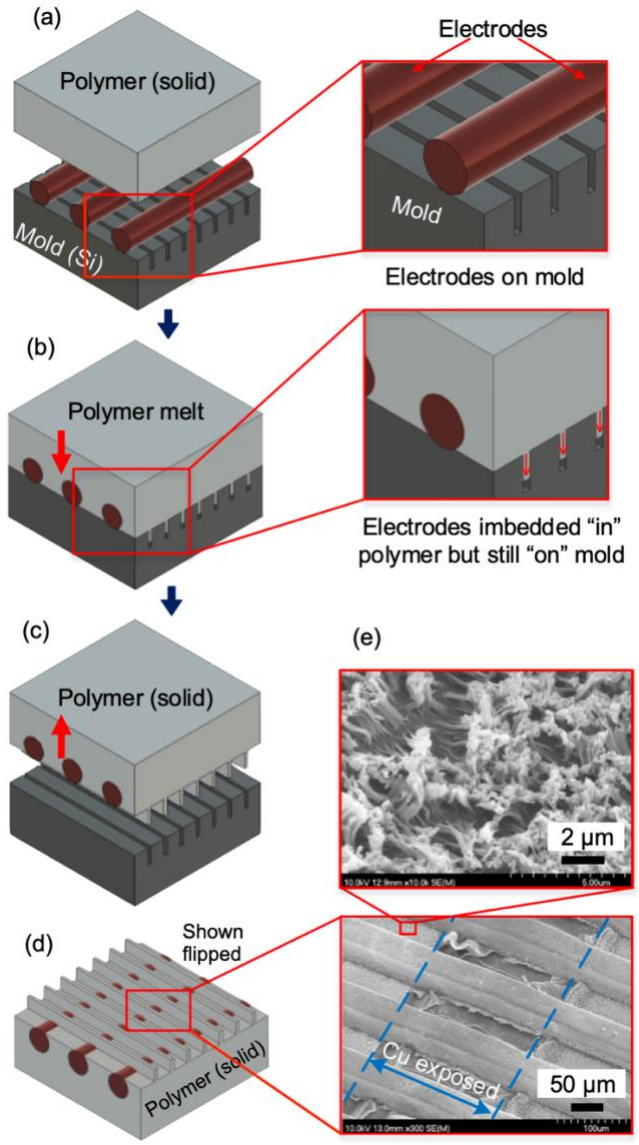

Fig. 3. One-step hot embossing process to make a semi-active SHPo surface with electrodes imbedded but exposed in microstructures. (a) Electrodes are sandwiched between mold and polymer film (Teflon FEP used). (b) The polymer is melted and flows past the electrodes into the microstructures (trenches used) on the mold while electrodes are pressed against and stay on the mold. (c) The polymer is cooled down and demolded. (d) Final surface (obtained here is a whole-Teflon SHPo film) with electrodes at the bottom of trenches. (e) SEM images of the SHPo surface showing an imbedded but exposed electrode and nanograss around it on the trench bottom.

The demolding step should be well-controlled to keep the integrity of the microstructures as studied before[38] and discussed in Supporting Information. A typical semi-active SHPo surface obtained by the above process is shown in Fig. 3(e), which shows the electrode imbedded underneath and exposed on the bottom surface of microtrenches. Furthermore, the inset SEM shows the "nanograss" on the bottom surface of the microtrenches. Molded from the nanoholes made on the top surface of the mold by a silver-assisted silicon etching (see the Supporting Information for details), the nanograss was proven critical for lateral gas propagation within the microtrenches that ensures plastron restoration with self-termination[31]. Compared with the smooth surface of Teflon FEP which has water receding contact angle <100°, the nanograss surface of Teflon FEP was estimated to have >150°, significantly promoting the lateral gas expansion. Moreover, the nanograss tended to stay locally dewetted even when the

microtrenches were wetted, thanks to its nanoscale structural pitch[16], which may help fight contamination or biofouling under practical conditions. Lastly, it is worth noting that the entire fabrication process involves only one hot-embossing step scalable for mass-manufacturing despite the multi-functionalities on the device, i.e., (i) trench geometry being very large and deep (both in ~100 μm range) to provide an appreciable drag reduction[36] and ensure plastron restoration[31], (ii) bottom surface of trenches covered with nanograss but nowhere else[31-32], and (iii) metal electrodes imbedded underneath but exposed on the bottom surface of trenches.

SELF-POWERED SURFACE FABRICATED BY ONE-STEP MOLDING

The developed hot-embossing process has been used to fabricate the proposed semi-active SHPo surfaces larger than ~1 cm x 1 cm in size and containing 40 trenches with 100 μm pitch, 50% gas fraction, 150 μm depth (i.e., grating height), and 1 cm length – much larger than the single trench sample of Fig. 2 (~1 mm x 4 mm in size with 1 mm long trench). Copper and magnesium were used as cathode and anode material, respectively, in this device. The standard electrode potentials of magnesium and water are, again, −2.37 V[34] and −0.83 V[34], respectively, while the activation overpotential of hydrogen evolution on copper is ~0.14 V[39]. Since the overall cell potential of 1.54 V is higher than the overpotential for hydrogen evolution on copper electrode (~0.14 V), spontaneous hydrogen generation is ensured. Following the two different electrode arrangements shown in Figs. 1(b, c), two different plastron-restoration samples were fabricated and tested in seawater. Although successful, the results for Fig. 1(b) is presented in the Supporting Information with Fig. S4 due to its secondary value. Realizing Fig. 1(c), the main sample had copper wires embedded underneath the microtrenches and a magnesium sheet outside the microtrenches, as shown schematically and with a picture in Fig. 4(a). The completed whole-Teflon sample was submerged in seawater to test the plastron restoration. When submerged initially as shown in the bottom picture of Fig. 4(a), the sample had the plastron appearing as dark horizontal lines. This is opposite to the usual silvery appearance reported on an opaque material, because the light from behind was seen through the transparent sample but reflected back by the water-air interfaces, making the plastron appear dark. The device was tested in seawater with the self-powered and self-regulated gas restoration process shown in Fig. 4(b) and Video S3. At t = 0 s, a number of trenches were flooded by squirting water with a pipette, and hydrogen was generated right away on the copper electrodes, verifying the self-powering and self-initiating nature of plastron restoration. The generated hydrogen then started to propagate along the microtrenches (e.g., t = 70 s) with no bubbles leaving the surface. The gas generation stopped when all trenches were refilled with gas practically everywhere (> 99% of area) (e.g., t = 100 s), verifying the self-terminating nature of plastron preservation. We have also explored samples as large as 4 cm x 4 cm, which is the wafer size used for the mold. While gas generation and propagation were confirmed in practically all trenches, the gas coverage (< 80% of area) was not satisfactory. The manual fabrication in research lab apparently lacked the level of uniformity and quality control needed to obtain large areas, calling for professionally prepared fabrication next. Furthermore, considering the large numbers of plastron-generation cycles expected for marine applications, long-term experiments to assess various secondary effects, such as the potential salt accumulation at anode (e.g., magnesium hydroxide), should be performed in future studies.

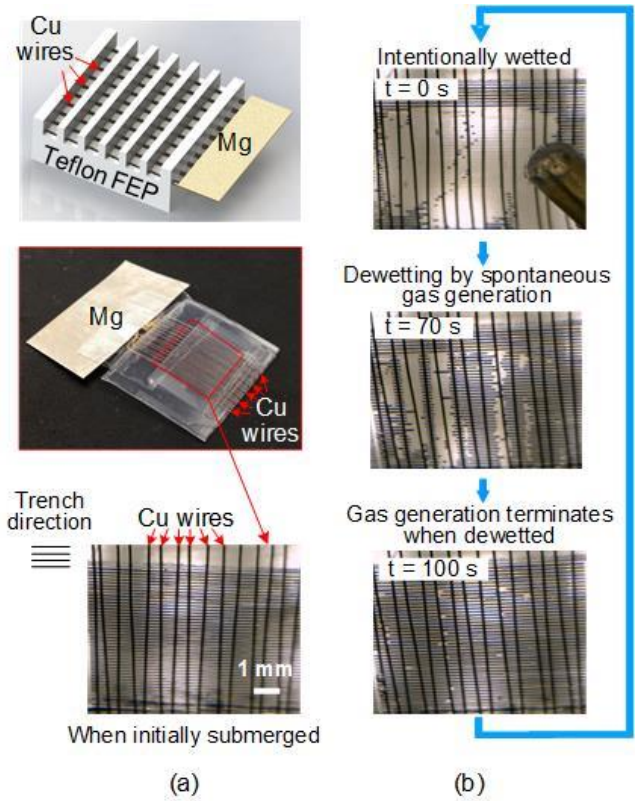

Fig. 4. Self-powered semi-active surface made by the one-step hot embossing process. (a) A schematic view and pictures of the whole-Teflon sample. (b) Plastron preservation process confirms the self-powering and self-regulation.

SUMMARY

We have proposed and confirmed a self-powered SHPo surfaces that restore lost plastron in a self-regulated manner. A one-step hot embossing process has been developed to fabricate semi-active SHPo surfaces out of a Teflon FEP film. Although successfully tested mostly with relatively small samples (1 cm x 1 cm), the developed fabrication is scalable for large areas and mass manufacturing. The self-powered plastron restoring mechanism made the semi-active SHPo surface easier to deploy, and the one-step molding process allowed the semi-active SHPo surface to be large and of low cost, together breaking two major bottlenecks toward real-world applications.

ACKNOWLEDGEMENTS

This research has been funded by DARPA HR0011-15-2-0021 and NSF 1336966 as well as UCLA Graduate Fellowship (C.L.) and Volgenau Endowed Chair in Engineering (C.-J.K.). The authors thank Guangyi Sun for his advice on mold fabrication.

REFERENCES

1. Betz, A. R.; Jenkins, J.; Kim, C.-J.; Attinger, D. Boiling Heat Transfer on Superhydrophilic, Superhydrophobic, and Superbiphilic Surfaces. *Int. J. Heat Mass Transf.* **2013,** *57* (2), 733-741. DOI: 10.1016/j.ijheatmasstransfer.2012.10.080

2. Tian, C.; Wang, X.; Liu, Y.; Yang, W.; Hu, H.; Pei, X.; Zhou, F. In Situ Grafting Hydrophilic Polymeric Layer for Stable Drag Reduction. *Langmuir* **2019,** *35* (22), 7205-7211. DOI: 10.1021/acs.langmuir.9b00321
3. Rothstein, J. P. Slip on Superhydrophobic Surfaces. *Annu. Rev. Fluid Mech.* **2010,** *42*, 89-109. DOI: 10.1146/annurev-fluid-121108-145558
4. Choi, C.-H.; Kim, C.-J. Large Slip of Aqueous Liquid Flow over a Nanoengineered Superhydrophobic Surface. *Phys. Rev. Lett.* **2006,** *96* (6), 066001. DOI: 10.1103/Physrevlett.96.066001
5. Xu, M.; Grabowski, A.; Yu, N.; Kerezyte, G.; Lee, J.-W.; Pfeifer, B. R.; Kim, C.-J. Superhydrophobic Drag Reduction for Turbulent Flows in Open Water. *Physical Review Applied* **2020,** *13* (3), 034056. DOI: 10.1103/PhysRevApplied.13.034056
6. Arnott, J.; Wu, A. H.; Vucko, M. J.; Lamb, R. N. Marine Antifouling from Thin Air. *Biofouling* **2014,** *30* (9), 1045-1054. DOI: 10.1080/08927014.2014.967687
7. Brocher, F. Recherches Sur La Respiration Des Insectes Aquatiques Adultes. L'hydrophile. *Ann. Biol. Lacustre* **1912,** *5*, 136.
8. Barthlott, W.; Schimmel, T.; Wiersch, S.; Koch, K.; Brede, M.; Barczewski, M.; Walheim, S.; Weis, A.; Kaltenmaier, A.; Leder, A. The Salvinia Paradox: Superhydrophobic Surfaces with Hydrophilic Pins for Air Retention under Water. *Adv. Mater.* **2010,** *22* (21), 2325-2328. DOI: 10.1002/adma.200904411
9. Hinton, H. Plastron Respiration in Marine Insects. *Nature* **1966,** *209* (5019), 220-221. DOI: 10.1111/j.1469-185X.1950.tb01590.x
10. Poetes, R.; Holtzmann, K.; Franze, K.; Steiner, U. Metastable Underwater Superhydrophobicity. *Phys. Rev. Lett.* **2010,** *105* (16), 166104. DOI: 10.1103/PhysRevLett.105.166104
11. Lv, P.; Xue, Y.; Shi, Y.; Lin, H.; Duan, H. Metastable States and Wetting Transition of Submerged Superhydrophobic Structures. *Phys. Rev. Lett.* **2014,** *112* (19), 196101. DOI: 10.1103/PhysRevLett.112.196101
12. Seo, J.; García-Mayoral, R.; Mani, A. Turbulent Flows over Superhydrophobic Surfaces: Flow-Induced Capillary Waves, and Robustness of Air–Water Interfaces. *J. Fluid Mech.* **2018,** *835*, 45-85. DOI: 10.1017/jfm.2017.733
13. Wexler, J. S.; Jacobi, I.; Stone, H. A. Shear-Driven Failure of Liquid-Infused Surfaces. *Phys. Rev. Lett.* **2015,** *114* (16), 168301. DOI: 10.1103/PhysRevLett.114.168301
14. Bocquet, L.; Lauga, E. A Smooth Future? *Nat. Mater.* **2011,** *10* (5), 334-337. DOI: 10.1038/nmat2994
15. Hokmabad, B. V.; Ghaemi, S. Effect of Flow and Particle-Plastron Collision on the Longevity of Superhydrophobicity. *Sci. Rep.* **2017,** *7*, 41448. DOI: 10.1063/1.5064817
16. Xu, M.; Sun, G.; Kim, C.-J. Infinite Lifetime of Underwater Superhydrophobic States. *Phys. Rev. Lett.* **2014,** *113* (13), 136103. DOI: 10.1103/PhysRevLett.113.136103
17. Peaudecerf, F. J.; Landel, J. R.; Goldstein, R. E.; Luzzatto-Fegiz, P. Traces of Surfactants Can Severely Limit the Drag Reduction of Superhydrophobic Surfaces. *Proc. Natl. Acad. Sci. U.S.A.* **2017,** *114* (28), 7254-7259. DOI: 10.1073/pnas.1702469114
18. Lee, C.; Choi, C.-H.; Kim, C.-J. Superhydrophobic Drag Reduction in Laminar Flows: A Critical Review. *Exp. Fluids* **2016,** *57* (12), 176. DOI: 10.1007/s00348-016-2264-z
19. Lee, Y. W.; Park, S. H.; Kim, K. B.; Lee, J. K. Fabrication of Hierarchical Structures on a Polymer Surface to Mimic Natural Superhydrophobic Surfaces. *Adv. Mater.* **2007,** *19* (17), 2330-2335. DOI: 10.1002/adma.200700820
20. Lee, C.; Kim, C.-J. Maximizing the Giant Liquid Slip on Superhydrophobic Microstructures by Nanostructuring Their Sidewalls. *Langmuir* **2009,** *25* (21), 12812-12818. DOI: 10.1021/la901824d
21. Hensel, R.; Helbig, R.; Aland, S.; Braun, H. G.; Voigt, A.; Neinhuis, C.; Werner, C. Wetting Resistance at Its Topographical Limit: The Benefit of Mushroom and Serif T Structures. *Langmuir* **2013,** *29* (4), 1100-1112. DOI: 10.1021/la304179b
22. Liu, T. L.; Kim, C.-J. Turning a Surface Superrepellent Even to Completely Wetting Liquids. *Science* **2014,** *346* (6213), 1096-1100. DOI: 10.1126/science.1254787
23. Carlborg, C. F.; van der Wijngaart, W. Sustained Superhydrophobic Friction Reduction at High Liquid Pressures and Large Flows. *Langmuir* **2011,** *27* (1), 487-493. DOI: 10.1021/La103624d

24. Wong, T.-S.; Kang, S. H.; Tang, S. K. Y.; Smythe, E. J.; Hatton, B. D.; Grinthal, A.; Aizenberg, J. Bioinspired Self-Repairing Slippery Surfaces with Pressure-Stable Omniphobicity. *Nature* **2011,** *477* (7365), 443-447. DOI: 10.1038/nature10447
25. Fukuda, K.; Tokunaga, J.; Nobunaga, T.; Nakatani, T.; Iwasaki, T.; Kunitake, Y. Frictional Drag Reduction with Air Lubricant over a Super-Water-Repellent Surface. *J. Mar. Sci. Technol.* **2000,** *5* (3), 123-130. DOI: 10.1007/s007730070009
26. Ceccio, S. L. Friction Drag Reduction of External Flows with Bubble and Gas Injection. *Annu. Rev. Fluid Mech.* **2010,** *42*, 183-203. DOI: 10.1146/annurev-fluid-121108-145504
27. Simovich, T.; Rosenhahn, A.; Lamb, R. N. Thermo-Regeneration of Plastrons on Superhydrophobic Coatings for Sustained Antifouling Properties. *Adv. Eng. Mater.* **2019,** *22*, 1900806. DOI: 10.1002/adem.201900806
28. Saranadhi, D.; Chen, D.; Kleingartner, J. A.; Srinivasan, S.; Cohen, R. E.; McKinley, G. H. Sustained Drag Reduction in a Turbulent Flow Using a Low-Temperature Leidenfrost Surface. *Science Advances* **2016,** *2* (10), e1600686. DOI: 10.1126/sciadv.1600686
29. Vakarelski, I. U.; Chan, D. Y.; Thoroddsen, S. T. Leidenfrost Vapour Layer Moderation of the Drag Crisis and Trajectories of Superhydrophobic and Hydrophilic Spheres Falling in Water. *Soft Matter* **2014,** *10* (31), 5662-5668. DOI: 10.1039/c4sm00368c
30. McCormick, M. E.; Bhattacharyya, R. Drag Reduction of a Submersible Hull by Electrolysis. *Nav. Eng. J.* **1973,** *85* (2), 11-16. DOI: 10.1111/j.1559-3584.1973.tb04788.x
31. Lee, C.; Kim, C.-J. Underwater Restoration and Retention of Gases on Superhydrophobic Surfaces for Drag Reduction. *Phys. Rev. Lett.* **2011,** *106* (1), 14502. DOI: 10.1103/PhysRevLett.106.014502
32. Lee, C.; Kim, C.-J. Wetting and Active Dewetting Processes of Hierarchically Constructed Superhydrophobic Surfaces Fully Immersed in Water. *J. Microelectromech. Syst.* **2012,** *21* (3), 712-720. DOI: 10.1109/Jmems.2012.2184081
33. Freeman, R.; Houck, A. C.; Kim, C.-J. Visualization of Self-Limiting Electrochemical Gas Generation to Recover Underwater Superhydrophobicity. In *Proceedings of the 18th International Conference on Solid-State Sensors, Actuators and Microsystems*, Anchorage, AK, U.S.A., June 2015, pp 1818-1821. DOI: 10.1109/TRANSDUCERS.2015.7181301
34. Vanýsek, P. Electrochemical Series. *Handbook of Chemistry and Physics* **2012,** *93*, 5-80.
35. Gong, M.; Zhou, W.; Tsai, M.-C.; Zhou, J.; Guan, M.; Lin, M.-C.; Zhang, B.; Hu, Y.; Wang, D.-Y.; Yang, J. Nanoscale Nickel Oxide/Nickel Heterostructures for Active Hydrogen Evolution Electrocatalysis. *Nat. Commun.* **2014,** *5* (1), 1-6. DOI: 10.1038/ncomms5695
36. Park, H.; Sun, G.; Kim, C.-J. Superhydrophobic Turbulent Drag Reduction as a Function of Surface Grating Parameters. *J. Fluid Mech.* **2014,** *747*, 722-734. DOI: 10.1017/jfm.2014.151
37. Woolford, B.; Prince, J.; Maynes, D.; Webb, B. W. Particle Image Velocimetry Characterization of Turbulent Channel Flow with Rib Patterned Superhydrophobic Walls. *Phys. Fluids* **2009,** *21* (8), 085106. DOI: 10.1063/1.3213607
38. Dirckx, M. Demolding of Hot Embossed Polymer Microstructures. Doctoral Thesis, Massachusetts Institute of Technology, MA, 2010.
39. Wood, R. J. K.; Fry, S. A. The Synergistic Effect of Cavitation Erosion and Corrosion for Copper and Cupro-Nickel in Seawater. *J. Fluids Eng.* **1989,** *111*, 271-277. DOI: 10.1115/1.3243641